J. Cent. South Univ. (2017) 24: 1263−1268
DOI: 10.1007/s11771-017-3530-9

Springer

An elasto-visco-plastic constitutive model of polypropylene incorporating craze damage behavior and its validation

GUI Zhong-xiang(桂中祥)[1, 2], HU Xiao(胡肖)[2], WANG Zi-jian(王子健)[2]

1. The 38th Research Institute of China Electronics Technology Group Corporation, Hefei 230088, China;
2. State Key Laboratory of Materials Processing and Die & Mould Technology, Huazhong University of Science and Technology, Wuhan 430074, China

Abstract: An elasto-visco-plastic constitutive model incorporating the craze damage behavior was developed for the polypropylene (PP), by using the plastic failure model applied for the concrete, to capture the craze yielding and stress-whitening phenomena. In addition, the developed constitutive model was implemented into finite element codes in Abaqus to simulate the tensile deformation. The standard uniaxial tensile tests were carried out. The stress−strain curves from the uniaxial tensile tests show that the stress keeps decreasing after yielding and the yield stress rises with the increasing of the strain rate. It is worth noting that the craze damage is more visible with higher strain rate. The stress-whitening can be seen clearly around the fracture. The uniaxial tensile tests using specially designed specimen with circular holes weakening were performed for the validation of the developed model. The simulation results of the tensile deformation of the hole-weakened specimen suggest that the stress-whitening could be attributed to the equivalent visco-plastic strain. By comparing between the simulation analysis and the experimental results, the proposed model can describe the stress whitening phenomenon with good accuracy.

Key words: elasto-visco-plastic constitutive model; craze yielding; stress-whitening; finite element implementation

1 Introduction

Nowadays, increasing attention is taking on the safety performance of vehicles. As one of the most significant safety factors, the dashboard above the supplementary restraint system is urged to meet the safety requirements during the crash of vehicles [1]. Polypropylene (PP) is commonly used for automotive dashboard, and its mechanical behavior has been widely studied [2−6]. Because of the visco-plasticity behavior of PP [7], its mechanical properties are significantly influenced by the temperature and the strain rate. It is necessary to investigate the complicate mechanical response of PP.

The damage and failure behavior of solid polymers [8−11] and the mechanical behavior at high strain rates [12−14] is studied by experiments. In addition, several constitutive models were established to predict the complicated mechanical behaviors of thermoset and thermoplastic materials by computer aided calculations. For example, the constitutive model such as hyper-elastic models [15−18] and elasto-plastic models [19−22] were implemented into finite element analysis software [23] to describe the strain rate and temperature-dependent behavior of polymers. As for these generic models, precise results may not be easily obtained for a specific material, and a series of customized experiments to determine parameters are always required. This inconvenience can be avoided by implementing the mathematical models which can be written for specific material behavior into user-defined subroutines [24]. However, this solution demands additional programming process and compiling software.

Generally, most of the existing models are the mathematical expressions of the stress strain curves from the tensile tests, without taking specific physical phenomena into consideration. A mechanism based elasto-visco-plastic constitutive model using plastic failure model incorporating the craze damage behavior was proposed in this work. Moreover, the developed constitutive model was implemented into the finite element codes of Abaqus. And the model parameters were optimized by minimizing the difference between the experimental observation from the uniaxial tensile tests using both standard and special designed specimens and that predicted by the model.

Foundation item: Project(51275185) supported by the National Natural Science Foundation of China
Received date: 2016−02−25; **Accepted date:** 2017−06−19
Corresponding author: GUI Zhong-xiang, PhD; +86−13856951081; E-mail: gxiang518@163.com

2 Constitutive and damage model

2.1 Elasto-visco-plastic constitutive model

When an external load is exerted on a material, the yielding and plastic flow will occur as the stress reaches a critical value. If the plastic flow is related to the strain rate, the material can be defined as a visco-plastic material. Further, the visco-plastic behavior of the material could be described by the combination of a viscous component and a plastic component. If the material presents the viscous flow behavior only after the stress reaches the yield limit, then it could be regard as rigid before the yielding, thereby this feature can be described by the viscous component and the plastic component in the parallel connection manner, which is referred as Bingham media. And its constitutive relation under uniaxial stress state is

$$\begin{cases}\sigma=\sigma_k+\eta\dot{\varepsilon},\sigma>\sigma_k\\ \dot{\varepsilon}=0,\sigma<\sigma_k\end{cases} \tag{1}$$

where σ, σ_k, η and $\dot{\varepsilon}$ represent the instant stress, critical stress, viscosity coefficient and strain rate, respectively.

The material model could be generally expressed by three components, i.e. the spring, viscous and plastic component, if the elastic deformation of the material can be ignored. Moreover, it can be divided into viscous-elasto-plastic model and elastic-visco-plastic model, according to the viscosity effects. The former takes the viscous effects into consideration at the elastic deformation stage as well as the plastic stage; while the latter ignores viscous effects in the elastic stage, which means the viscous component only works after the yield. Based on the Bingham media theory mentioned above, an elastic component is added in series way, this paper describes the performance of PP with the elastic-visco-plastic model shown in Fig. 1. Its uniaxial stress state can be described as follows.

The total strain of the model shown in the Fig. 1 is

$$\varepsilon=\varepsilon^{\mathrm{e}}+\varepsilon^{\mathrm{vp}} \tag{2}$$

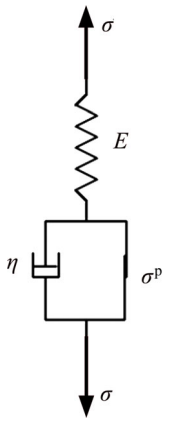

Fig. 1 Elasto-visco-plastic model

where ε^{e} is the elastic strain component and $\varepsilon^{\mathrm{vp}}$ is the visco-plastic strain component.

Because the model is in series, the stress of the spring element is equal to the total stress. That is,

$$\sigma=\sigma^{\mathrm{e}}=E\varepsilon^{\mathrm{e}} \tag{3}$$

For an ideal plastic element, its stress value depends on whether the material stress reaches yielding. In addition, the stress level drive the plastic flow to proceed is related to the strengthening properties of material. For simplicity, it is assumed that the material is linear strengthened, and the strengthening parameters are defined as

$$H=\frac{\mathrm{d}\sigma}{\mathrm{d}\varepsilon^{\mathrm{p}}}\frac{\mathrm{d}\sigma}{\mathrm{d}\varepsilon-\mathrm{d}\varepsilon^{\mathrm{e}}} \tag{4}$$

The stress of the material after plastic yield is

$$\sigma^{\mathrm{p}}=\sigma_k+H\varepsilon^{\mathrm{p}}=\sigma_k+H\varepsilon^{\mathrm{vp}} \tag{5}$$

For the ideal plastic element,
when $\sigma<\sigma_{\mathrm{s}}$,

$$\sigma^{\mathrm{p}}=\sigma^{\mathrm{e}}=\sigma \tag{6}$$

while $\sigma>\sigma_{\mathrm{s}}$, it is

$$\sigma^{\mathrm{p}}=\sigma-\sigma^{\mathrm{v}}=\sigma-\eta\frac{\partial\varepsilon^{\mathrm{vp}}}{\partial t} \tag{7}$$

By taking Eq. (5) into Eq. (7), it yields

$$\sigma=\sigma_k+H\varepsilon^{\mathrm{vp}}+\eta\frac{\partial\varepsilon^{\mathrm{vp}}}{\partial t} \tag{8}$$

Considering Eqs. (2), (3), (5) and (7), there is

$$HE\varepsilon+\eta E\frac{\partial\varepsilon}{\partial t}=H\sigma+E\left(\sigma-\sigma_k\right)+\eta\frac{\partial\sigma}{\partial t} \tag{9}$$

Give a final formula,

$$\dot{\varepsilon}=\frac{\dot{\sigma}}{E}+\frac{1}{\eta}\left[\sigma-\left(\sigma_k+H\varepsilon^{\mathrm{vp}}\right)\right] \tag{10}$$

where $\dot{\varepsilon}^{\mathrm{e}}=\dfrac{\dot{\sigma}}{E}$ means the elastic strain increment.

Combined with Eq. (2), the visco-plastic strain rate could be expressed as

$$\dot{\varepsilon}^{\mathrm{vp}}=\frac{1}{\eta}\left[\sigma-\left(\sigma_k+H\varepsilon^{\mathrm{vp}}\right)\right] \tag{11}$$

The above equation shows that the visco-plastic strain rate is determined by the stress beyond the yield stress. Furthermore, the steady-state yield stress could be obtained from the stress−strain curves under steady state.

The Bingham media mentioned above is the simplest visco-plastic model. Based on the assumption that the plastic strain rate is in direct portion to the stress

difference between the stress instant stress and the stress sites at static curve, i.e., overstress, MALVERN proposed the following model:

$$\dot{\varepsilon}=\frac{\dot{\sigma}}{E}+\left\langle \Phi\left[\sigma-f\left(\varepsilon\right)\right]\right\rangle \tag{12}$$

where E is the elastic modulus, $f(\varepsilon)$ is the material stress during static stretching, σ is the stress in consideration of the strain rate, and for different materials function there are different forms of Φ. $\langle\Phi\rangle$ is defined as

$$\begin{cases}\langle\Phi\rangle=\Phi, \sigma>f\left(\varepsilon\right)\\ \langle\Phi\rangle=0, \sigma<f\left(\varepsilon\right)\end{cases} \tag{13}$$

MALVERN discussed two different types of Φ: linear function and exponential function.

The linear function is

$$\Phi=c\left[\sigma-f\left(\varepsilon\right)\right] \tag{14}$$

While the exponential function is

$$\Phi=a\left\{\exp b\left[\sigma-f\left(\varepsilon\right)\right]-1\right\} \tag{15}$$

where a, b and c are material constants determined by the experimental results.

HOHENEMSER and PRAGER give the visco-plastic material constitutive equation through analogy:

$$2\eta\dot{\varepsilon}_{ij}^{\mathrm{p}}=2k\left\langle F\right\rangle\frac{\partial F}{\partial\sigma_{ij}} \tag{16}$$

where $F=\dfrac{\sqrt{J_2}}{k}-1=\dfrac{\sqrt{\dfrac{1}{2}s_{ij}s_{ij}}}{k}-1$, s_{ij} is partial stress components, $\dot{\varepsilon}_{ij}^{\mathrm{p}}$ is non-elastic strain rate, η is viscous coefficient, k is shear yield strength, J_2 is second invariant of deviator stress, and $\langle F\rangle$ is defined as

$$\begin{cases}\langle F\rangle=F, F>0\\ \langle F\rangle=0, F\le 0\end{cases} \tag{17}$$

PERZYNA developed the above H-P equation as Perzyna equation:

$$\dot{\varepsilon}_{ij}=\frac{1}{2G}\dot{s}_{ij}+\frac{1-2\nu}{E}\dot{\sigma}_{kk}\delta_{ij}+\gamma\left\langle\Phi(F)\right\rangle\frac{\partial f}{\partial\sigma_{ij}} \tag{18}$$

where

$$\begin{cases}\left\langle\Phi\left(F\right)\right\rangle=F, F>0\\ \left\langle\Phi\left(F\right)\right\rangle=0, F\le 0\end{cases} \tag{19}$$

If $\Phi(F)$ is taken as an expression of hardening function σ_x, there is

$$\Phi(F)=F^n=\left(\frac{\sqrt{J_2}}{\sigma_x}-1\right)^n \tag{20}$$

when n=1 and $\sigma_x=\sigma_k$, Eq. (18) becomes

$$\dot{\varepsilon}_{ij}=\frac{1}{2G}\dot{s}_{ij}+\frac{1-2\nu}{E}\dot{\sigma}_{kk}\delta_{ij}+\gamma\left(\frac{\sqrt{J_2}}{\sigma_k}-1\right)\frac{\partial f}{\partial\sigma_{ij}} \tag{21}$$

Given that $\eta=\dfrac{\sigma_k}{\gamma}$, and $\dfrac{\partial f}{\partial\sigma_{ij}}=\dfrac{s_{ij}}{2\sqrt{J_2}}$, Eq. (21) transforms to

$$\begin{cases}\dot{\varepsilon}_{ij}=\dfrac{1}{2G}\dot{s}_{ij}+\dfrac{1-2\nu}{E}\dot{\sigma}_{kk}\delta_{ij}+\dfrac{1-\dfrac{\sigma_k}{\sqrt{J_2}}}{2\eta}S_{ij}, \ \sqrt{J_2}>\sigma_k\\ \dot{\varepsilon}_{ij}=\dfrac{1}{2G}\dot{s}_{ij}+\dfrac{1-2\nu}{E}\dot{\sigma}_{kk}\delta_{ij}, \ \sqrt{J_2}<\sigma_k\end{cases} \tag{22}$$

2.2 Crazing damage model

There are two yield patterns of the polymer solids. The first is the shear yield, which is characterized by shear zone, and the shear band is preferentially oriented along the maximum shear direction. The second is the crazing yield, which is typical of stress-whitening. The crazing structure can be directly observed by an electron microscope. That structure is composed of cavities containing many micro-deformation region, and cavities matrix containing small fibers. The fibrils connect the two surfaces of crazes and fill approximately half of the crazing volume. There is greater density difference between the crazing and the matrix, resulting in a strong light scattering, at macro level stress-whitening [25]. The stress-whitening phenomenon of PP was observed obviously in plastic uniaxial tension (Fig. 2), and its main yield form is the craze yielding.

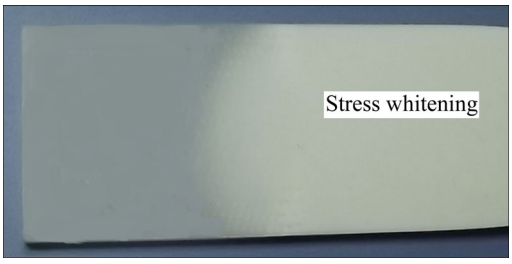

Fig. 2 Stress-whitening of PP under uniaxial tension

Figure 2 shows that, the overall loading area of the specimen did not change significantly, however, because of the crazing, the specimen fractured. It implies that as the same effect as the macro-necking, the craze is micro-necking according to its structural features, resulting in the loading area decreasing. It could be concluded that the crazing brings about that the yield stress decreased with the increasing strain (strain softening) and the elastic modulus reduction. According to the above arguments, the crazing damage of the PP is described by using the plastic failure model applied for the concrete.

The strain rate $\dot{\varepsilon}$ can be divided into elastic and inelastic components:

$$\dot{\varepsilon} = \dot{\varepsilon}^{\mathrm{e}} + \dot{\varepsilon}^{\mathrm{vp}} \tag{23}$$

In consideration of the impact of the damage on the material elasticity, stress−strain relationship is

$$\sigma = (1-d)\boldsymbol{D}_0^{\mathrm{e}}\left(\varepsilon - \varepsilon^{\mathrm{vp}}\right) = \boldsymbol{D}^{\mathrm{e}}\left(\varepsilon - \varepsilon^{\mathrm{vp}}\right) \tag{24}$$

where $\boldsymbol{D}_0^{\mathrm{e}}$ is the initial elastic matrix, $\boldsymbol{D}^{\mathrm{e}}$ is the elastic matrix after fracture, and d evaluates the damage degree, which is a function of inelastic equivalent strain $\bar{\varepsilon}^{\mathrm{vp}}$:

$$\mathrm{d}\left(\bar{\varepsilon}^{\mathrm{vp}}\right) = \frac{\bar{\varepsilon}^{\mathrm{vp}} - \bar{\varepsilon}_0^{\mathrm{vp}}}{\bar{\varepsilon}_{\mathrm{f}}^{\mathrm{vp}} - \bar{\varepsilon}_0^{\mathrm{vp}}} \tag{25}$$

where $\bar{\varepsilon}_0^{\mathrm{vp}}$ means the inelastic equivalent strain when the damage begins, $\bar{\varepsilon}_{\mathrm{f}}^{\mathrm{vp}}$ is the inelastic equivalent strain when the material is damaged completely, and $\bar{\varepsilon}^{\mathrm{vp}}$ is the current inelastic equivalent strain.

With the combination of both sectors above, an elasto-visco-plastic constitutive model with damage behavior was proposed in this work:

$$\begin{cases} \begin{cases} \dot{\sigma}_{ij} = 2G\left(\dot{\varepsilon}_{ij} - \dfrac{1-\sigma_k/\sqrt{J_2}}{2\eta}s_{ij}\right) + \dfrac{E\dot{\varepsilon}_{kk}}{3(1-2\nu)}\delta_{ij} \\ \sigma^{m+1} = (1-d)\left(\sigma^m + \Delta t\dot{\sigma}_{ij}\right) \end{cases}, \ \sqrt{J_2} > \sigma_k \\ \begin{cases} \dot{\sigma}_{ij} = 2G\dot{\varepsilon}_{ij} + \dfrac{E\dot{\varepsilon}_{kk}}{3(1-2\nu)}\delta_{ij}, \\ \sigma^{m+1} = (1-d)\left(\sigma^m + \Delta t\dot{\sigma}_{ij}\right) \end{cases}, \ \sqrt{J_2} < \sigma_k \end{cases} \tag{26}$$

where m means the incremental step and Δt is the time increment.

3 Experimental and simulation method

3.1 Materials and tensile tests

The PP homopolymer Grade T30S with its density of 0.9 g/cm^3 (manufacturer data) and melt flow index MFI of 4 g/10 min (for 230 °C, 2.16 kg according to ISO 1133) used in this work were supplied by Wuhan Petrochemical Co. (China). The samples for mechanical studies were prepared in the following way: samples were cut off from a thick film with 3 mm in thickness, obtained by compression moulding at temperature of 230 °C and cooled between metal plates. The samples were shaped according to ISO 527 standard. AG-IC 100 kN tensile testing machine was applied to test the tensile property of PP. Figure 3 shows the geometrical dimensions of the specimen, and Table 1 gives the corresponding value in details.

The deformation−load curve can be obtained from the tensile tests. According to it, corresponding stress−strain curves can be calculated:

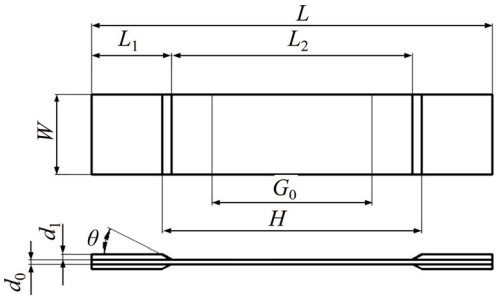

Fig. 3 Standard tensile specimen

Table 1 Parameters of specimen

Parameter	Value
Length, L/mm	250
Length of reinforcement, L_1/mm	150
Distance between reinforcements, L_2/mm	50
Distance between clamps, H/mm	170
Marked length, G_0/mm	100
Width, W/mm	50
Thickness, d_0/mm	3
Thickness of reinforcement, d_1/mm	3
Reinforcement angle, θ/(°)	30

$$\varepsilon = \ln\left(\frac{d_1}{l} + 1\right) \tag{27}$$

$$\sigma = \frac{F}{A} = \frac{F}{bh} \tag{28}$$

3.2 Finite element implementation

The developed elasto-visco-plastic constitutive model with damage behavior was written into the user subroutine in Abaqus by FORTRAN language. Meanwhile, the parameters required in the constitutive model were optimized by the experimental results (Table 2), thus making the simulation results more accurate and reliable. To be more specific, the actual stress−strain curves at different tensile rates were obtained during the tensile tests, which will be compared with the corresponding simulation results to optimize the simulation parameters.

Table 2 Parameters used in finite element analysis

E/MPa	σ_k/MPa	η/(MPa·s)	$\bar{\varepsilon}_0^{\mathrm{vp}}$	$\bar{\varepsilon}_{\mathrm{f}}^{\mathrm{vp}}$
1007	17.5	4.5	0.05	1.7

4 Results and discussion

4.1 Tensile tests results

Figure 4 shows the obtained stress−strain curves of the standard specimens at different strain rates. The yield

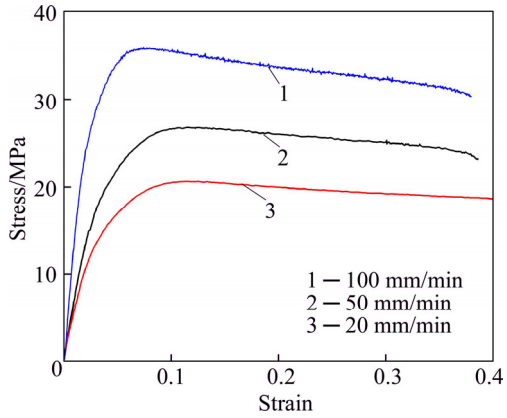

Fig. 4 Stress−strain curves at different tensile rates

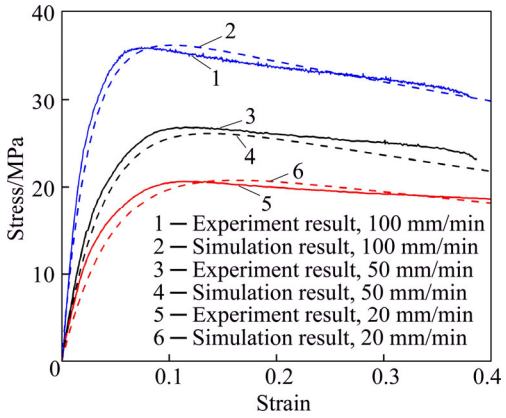

Fig. 5 Simulation results of tensile test compared with experimental ones

stress declines with the increased strain. Specially, it could be seen obviously that, the higher the tensile rate, the higher the yield stress, as well as the more visible the strain softening. When the stress level is less than 5 MPa, the three curves almost present the same slope. In addition, the stress-strain curve of the specimen deformed under tensile rate of 100 mm/s shows the maximum slope. When the stress state of PP reaches a critical state under external loads, it yields with rate dependent viscosity. In the necking region (after the yield point), structural transformation spherulite/fibrilla occurs. This new transformed structure which contains oriented crystalline and amorphous regions will greatly affect the plastic yielding of PP, which is a semi-crystalline polymer [25, 26]. In the uniaxial tensile test, PP yields in a form of crazing as shown in Fig. 2, which comprises quantities of cavities formed by micro-distortion. Stress-whitening is a visual sign of cavitation and caused by light scattering either by micro-voids or by assemblies of nano-voids [27, 28]. Figure 2 also indicates the whole bearing area of the specimen changes little; however, crazing actually reduces the bearing area of the material in a microscopic scale according to the characteristic of crazing yielding. Crazing acts in the similar way the macroscopic necking performs, which is characteristic of reduced yield stress and elasticity modulus with increased strain.

4.2 Numerical simulation results

The constitutive model proposed in constitutive and damage model section was implemented into the user subroutine for analysis by Abaqus to obtain the numerical simulation results of the tensile tests. Figure 5 shows the simulation results provided by the elasto-visco-plastic constitutive model with damage behavior proposed in this study fit well with the experimental results, proving the feasibility and accuracy of the developed model.

To further validate of the developed model, a tensile test of the specimen that has three circular weakening holes with a diameter of 1mm uniformly distributed along its width direction was designed (Fig. 6). Simulation was done to reveal the deformation. Figure 7(a) shows the equivalent visco-plastic strain distribution of the specimen before fracture, and Fig. 7(b) shows the stress-whitening of the fractured specimen. As can be seen from the comparison, the equivalent visco-plastic strain and the stress-whitening have shown the same distribution region. Thereby further confirms the equivalent visco-plastic strain led to the stress-whitening. Above all, the validation of the developed model was effectively proven once more.

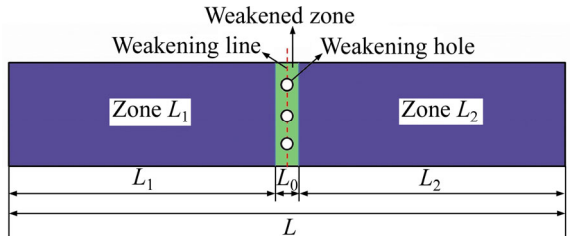

Fig. 6 Schematic diagram of weakened specimen

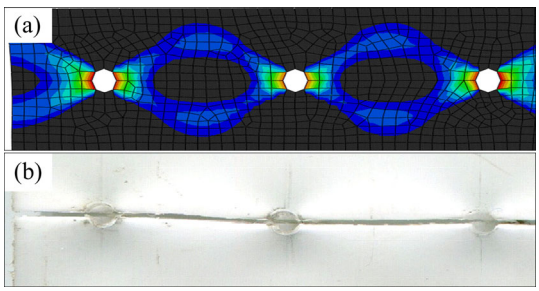

Fig. 7 Comparison between simulative and experimental results: (a) Strain distribution of hole-weakened specimen; (b) Stress-whitening of fractured specimen

5 Conclusions

1) Tensile test results of the standard specimens suggest that the flow behavior of PP material is sensitive to the strain rate. It exhibits visco-plasticity behavior.

The higher the strain rate is, the more remarkable the craze damage is, i.e. the occurrence of strain softening is more visible. The yield stress also increases with the increasing of the strain rate.

2) An elasto-visco-plastic constitutive model was proposed through analytical solution, by incorporating the plastic failure model applied for the concrete. Not only tensile test results of the standard specimens, but also those of the special designed ones show that the explored model can accurately predict the craze damage.

3) The comparison between the analytical solution of fracture mechanics and experimental results further validates the effectiveness and reliability of the developed elasto-visco-plastic constitutive model, in particular to present the stress-whitening phenomenon. In addition, the stress-whitening which is seen clearly around the fracture could be attributed to the equivalent visco-plastic strain.

References

[1] FLORENCE R, SHERMAN K. Trends driving design and materials changes in the instrument panel system [J]. SAE Technical Paper 970445, 1997, doi: 10.4271/970445.

[2] SERBAN D A, WEBER G, MARSAVINA L, SILBERSCHIMIDT V V, HUFENBACH W. Tensile properties of semi-crystalline thermoplastic polymers: Effects of temperature and strain rates [J]. Polymer Testing, 2013, 32(2): 413−425.

[3] HUANG J, RODRIGUEZ D. The effect of carbon nanotube orientation and content on the mechanical properties of polypropylene based composites [J]. Materials and Design, 2014, 55: 653−663.

[4] RIO T G, SALAZAR A, RODRIGUEZ J. Effect of strain rate and temperature on tensile properties of ethylene-propylene block copolymers [J]. Materials and Design, 2012, 42: 301−307.

[5] REIS J M L, PACKECO L J, da COSTA MATTOS H S. Tensile behavior of post-consumer recycled high-density polyethylene at different strain rates [J]. Polymer Testing, 2013, 32(2): 338−342.

[6] NUNES L C S, REIS J M L, da COSTA MATTOS H S. Parameters identification of polymer concrete using a fracture mechanics test method and full-field measurements [J]. Engineering Fracture Mechanics, 2011, 78(17): 2957−2965.

[7] BALIEUA R, LAUROA F, BENNANIA B, MOTTOLA E. A fully coupled elastoviscoplastic damage model at finite strains for mineral filled semi-crystalline polymer [J]. International Journal of Plasticity, 2013, 51: 241−270.

[8] TANG C Y, TSUI C P, SHEN W, LI C C, PENG L H. Modelling of non-linear stress-strain behaviour of HIPS with craze damage in tensile loading-unloading process [J]. Polymer Testing, 2000, 20(1): 15−27.

[9] ZARIA F, NAIT-ABDELAZIZA M, GLOAGUENB J M, LEFEBVREB J M. Modelling of the elasto-viscoplastic damage behaviour of glassy polymers [J]. International Journal of Plasticity, 2008, 24(6): 945−965.

[10] SELL C G, HIVER J M, DAHOUN A. Experimental characterization of deformation damage in solid polymers under tension, and its interrelation with necking [J]. International Journal of Solids and Structures, 2002, 39(13, 14): 3857−3872.

[11] BROWM E N, RAEP J, ORLER E B. The influence of temperature and strain rate on the constitutive and damage responses of polychlorotrifluoroethylene (PCTFE, Kel-F81) [J]. Polymer, 2006, 47(21): 7506−7518.

[12] JIANG Bing-yan, HU Jian-liang, LI Jun, LIU X C. Ultrasonic plastification speed of polymer and its influencing factors [J]. Journal of Central South University, 2012 (19): 380−383.

[13] SCHOBG M, BIEROEL C, GRELLMANN W, MECKLENBURG T. Mechanical behavior of glass-fiber reinforced thermoplastic materials under high strain rates [J]. Polymer Testing, 2008, 27(7): 893−900.

[14] MULLIKEN A D, BOYCE M C. Mechanics of the rate-dependent elastic-plastic deformation of glassy polymers from low to high strain rates. [J]. International Journal of Solids and Structures, 2006, 43(5): 1331−1356.

[15] KILLIAN H G, ENDERLE H F, UNSELD K. The use of the van der Waals model to elucidate universal aspects of structure-property relationships in simply extended dry and swollen rubbers [J]. Colloid & Polymer Science, 1986, 264(10): 866−876.

[16] MARLOW R S. A general first-invariant hyperelastic constitutive Model, in Constitutive Models for Rubber III [M]. London: Balkema Publishers, 2003.

[17] OGDEN R W. Large deformation isotropic elasticity−On the correlation of theory and experiment for incompressible tuberlike solids [J]. Proceedings of the Royal Society A, 1972, 326(1567): 565−584.

[18] RIVLIN R S, SAUNDERS D W. Large elastic deformations of isotropic materials. VII. Experiments on the deformation of rubber [J]. Philosophical Transactions of the Royal Society A, 1951, 251−288.

[19] NUNES L C S, DIAS F W R, da COSTA MATTOS H S. Mechanical behavior of polytetrafluoroethylene in tensile loading under different strain rates [J]. Polymer Testing, 2011, 30(7): 791−796.

[20] SERBAN D A, MARSAVINA L, SILBERSCHMIDT V. Behaviour of semi-crystalline thermoplastic polymers: Experimental studies and simulations [J]. Computational Materials Science, 2012, 52(1): 139−146.

[21] DUNNE F, PETRINIC N. Introduction to computational plasticity [M]. Oxford: Oxford University Press, 2006.

[22] REES D W A. Basic engineering plasticity [M]. Elsevier, 2006.

[23] Abaqus Analysis User's Manual [S].

[24] ROZANSKI A, GALESKI A. Plastic yielding of semicrystalline polymers affected by amorphous phase [J]. International Journal of Plasticity, 2013, 41: 14−29.

[25] HONG K, RASTOGI A, STROBL G. A Model treating tensile deformation of semicrystalline polymers: Quasi-static stress−strain relationship and viscous stress determined for a sample of Polyethylene [J]. Macromolecules, 2004, 37(26): 10165−10173.

[26] LIN J, SHENOGIN S, NAZARENKO S. Oxygen solubility and specific volume of rigid amorphous fraction in semicrystalline poly(ethylene terephthalate) [J]. Polymer, 2002, 43(17): 4733−4743.

[27] PAWLAK A, GALESKI A, ROZANSKI A. Cavitation during deformation of semicrystalline polymers [J]. Progress in Polymer Science, 2014, 39(5): 921−958.

[28] BARTCZAK Z, MORAWIEC J, GALESKI A. Structure and properties of isotactic polypropylene oriented by rolling with side constraints [J]. Journal of Applied Polymer Science, 2002, 86(6): 1413−1425.

(Edited by YANG Bing)

Cite this article as: GUI Zhong-xiang, HU Xiao, WANG Zi-jian. An elasto-visco-plastic constitutive model of polypropylene incorporating craze damage behavior and its validation [J]. Journal of Central South University, 2017, 24(6): 1263−1268. DOI: 10.1007/s11771-017-3530-9.